JOURNAL OF MATERIALS SCIENCE 32 (1997) 4821–4831

The hot compaction of SPECTRA gel-spun polyethylene fibre

R. J. YAN, P. J. HINE, I. M. WARD
IRC in Polymer Science and Technology, University of Leeds, Leeds LS2 9JT, UK
R. H. OLLEY, D. C. BASSETT
J. J. Thomson Physical Laboratory, Whiteknights, Reading RG6 6AF, UK

The compaction of gel-spun high molecular weight polyethylene (PE) fibre, SPECTRA 1000, has been investigated for a range of compaction temperatures between 142 °–155 °C. Differential scanning calorimetry (DSC), scanning electron microscopy (SEM) and broad-line nuclear magnetic resonance (NMR) techniques have been used to examine the structure of the compacted materials and to determine the compaction mechanisms. With increasing compaction temperature, the flexural properties of the compacted materials did not show any significant change up to 154 °C, but large changes were observed if the temperature was increased from 154 to 155 °C. DSC and SEM studies revealed that no evident surface melting and recrystallization occurred during hot compaction in the temperature range 144–154 °C, although the rigid crystalline fraction measured by NMR for all compacted materials is significantly lower than that for the original fibre. Significant transverse strength is also developed at the lower compaction temperatures, and this also only markedly increases on going from 154 to 155 °C. Structural investigations show how the fibres deform so as to interlock, and localized welding occurs, so as to bond each fibre to its neighbour. This is distinct from the melting and recrystallization at the surface of the fibres previously observed in melt spun fibres.

1. Introduction

Recent research at Leeds University [1] has shown that hot compaction of melt-processable fibres can be used to produce a fibre reinforced polyethylene/polyethylene composite retaining a very large proportion of the original fibre properties. Morphological studies at the University of Reading have shown that for those melt-spun polyethylene fibres, the fibres are bonded by a matrix phase consisting of recrystallized material melted on the surface of the fibres during the compaction process [2]. Hot compaction has been demonstrated and analysed in some detail for the melt-spun and drawn high modulus polyethylene (PE) fibres (Formerly known as TENFOR from SNIA fibre, Italy, but now known as CERTRAN from Hoechst Celanese, USA), [3, 4] but has also been applied with varying success to a wide range of melt-processable fibres including polyethylene terephthalate (PET) [5], polypropylene (PP) [6] and liquid crystalline polymer (VECTRAN).

In the case of TENFOR fibres after compaction under optimum conditions, at least 80% of the initial fibre properties can be retained; the density of the compacted product is very close to that of the original fibre, while the interfacial bonding developed through surface melting of the fibres is such that failure occurs in the original fibres rather than at the interface between the fibres and the recrystallized matrix. Compaction of PET fibres can also produce a composite material retaining a high proportion of the original fibre properties and adequate transverse strength. However electron microscopy studies reveal that good inter-fibre bonding is more difficult to achieve for PET fibres [5] than for the melt spun PE fibres [2, 4].

The high modulus, high strength gel-spun polyethylene fibres [7] represent another technology, which has been commercialized by DSM and Allied Signal, to produce DYNEEMA and SPECTRA fibres respectively. In this publication a study of the hot compaction of SPECTRA fibres is presesnted. A particular issue addressed is the relationship between the retention of fibre mechanical properties after hot compaction at different temperatures and the proportion of fibre melted and recrystallized. It will be shown that a combination of broad-line nuclear magnetic resonance (NMR) and differential scanning calorimetry (DSC) measurements provides valuable insight into this issue. Further definitive information on the morphological changes which occur on hot compaction has been obtained from electron microscopy of etched samples, where the comparison with previous results for compacted melt spun fibres is very informative.

0022–2461

2. Experimental procedure

2.1. Hot compacted sample preparation

The gel-spun PE fibres, with the commercial name SPECTRA 1000, were unidirectionally wound around a frame, and arranged in a parallel configuration in a matched metal mould which was placed in a heated compression press maintained at the required compaction temperature. The temperature of the fibre assembly was monitored by a thermocouple in the mould. A pressure of 2.8 MPa (400 p.s.i) was applied and the sample left for 10 min once it had reached the compaction temperature. This initial compact pressure is significantly higher than that employed in previous work on melt spun polyethylene fibres, 0.7 MPa (100 p.s.i.), and is required to restrain the gel spun fibres from shrinking. After a dwell time of 10 min, a higher pressure of 12.1 MPa (1700 p.s.i.) was applied for 1 min, following which the sample was quickly cooled to 100 °C. Finally the sample was removed from the press and allowed to cool in air.

2.2. Shrinkage

Shrinkage measurements were carried out on 30 cm long bundles of the macrofibres suspended in silicone oil. The variation in the length of the fibres was measured after the fibres had remained in the oil at the appropriate temperature for 10 min. Shrinkage is defined as the relative change in fibre length $\Delta l/l_0 \times 100\%$, l_0 being the initial fibre length at room temperature.

2.3. Differential scanning calorimetry (DSC)

The melting behaviour of the original fibre and the compacted materials was investigated using a Perkin-Elmer DSC-7 Series differential scanning calorimeter; the heating rate for all the tests was 10 °C min^{-1}.

To examine the effect of constraint on the melting behaviour of the original SPECTRA 1000 fibre, fibres were constrained either by two clamped DSC pans (resulting in so called "partially constrained" samples as the fibres tend to pull in from between the clamped pan lids during melting) or by winding the fibres around a small I-shaped frame of aluminium (so called "fully constrained" samples). Although at first sight the partially constrained condition would seem redundant, it was envisaged that this would most closely represent the constrained conditions seen during the DSC experiments on the compacted material themselves, as they cannot be constrained within the DSC pans but are obviously under partial constraint by virtue of the fibre to fibre bonding developed during compaction.

2.4. Mechanical analysis

The mechanical properties of the compacted materials were measured under three-point bend conditions using an Instron tensile testing machine. A crosshead speed of 1 mm min^{-1} and specimen width of 5 mm and thickness 2.0 mm were used. For measuring the longitudinal bending modulus, samples were cut parallel to the fibre direction, and tested using a bending span of 40 mm. To measure the transverse modulus and transverse strength, samples were cut perpendicular to the main fibre direction, and were tested using a bending span of 30 mm.

The longitudinal Young's modulus of the original fibre was measured on an Instron tensile testing machine using a gauge length of 200 mm and a crosshead speed of 1 mm $min.^{-1}$

2.5. Scanning electron microscopy (SEM)

For each specimen, a surface at 45 ° to the fibre direction was cut with glass knives when cooled with liquid nitrogen on an RMC cryo-ultramicrotome. The specimen was then etched for 2 h in a 1% solution of potassium permanganate in a mixture of 2 volumes of concentrated sulphuric acid and 1 volume dry orthophosphoric acid [8]. The etched cut surfaces were coated with gold and examined under a Philips SEM 515 scanning electron microscope. The photographs are of specimens tilted so as to observe directly down the fibre axis.

2.6. NMR measurements

The broad-line NMR tests were performed using a Varian DP60 Spectrometer operated at 60 MHz. A time averaging computer was used to add together the signals from the successive sweeps (sweep number = 60) through the spectrum to improve the signal to noise ratio.

The original fibres were firstly wound around a thin rod. Then they were taken off the rod and pressed into a strip. The strip was carefully put into the 4.5 mm diameter sample tube so that the fibres could be arranged parallel to the main magnetic field H. The angle between the fibre and H was not very precise due to the limits of the mounting method. The NMR sample was a square rod 40 mm long and a cross-section of 2.2×3.8 mm^2, which was cut from the compacted material along the transverse direction. The modulation field amplitude was 3.9×10^{-5} T and the average field interval at which the signal was recorded was about 5×10^{-6} T. All the results presented in this paper are from samples of fibres or compacted materials, aligned so that the main fibre direction was parallel to the magnetic field.

2.7. Calculation of crystallinity from NMR spectra

The following procedure developed at Leeds University [9] was employed to calculate the sample crystallinity from the broad line NMR spectra. The proton NMR signal from polyethylene can be considered as the superposition of two components, a broad component associated with the rigid crystalline regions and a narrow component associated with more mobile non-crystalline materials. Pranadi and Manuel [10] have proposed that the crystalline regions give rise to an NMR signal which can be modelled as a doublet in

which the two components have a Gaussian line shape. The Gaussian doublet line can then be defined by the following equation:

$$Y(\Delta H) = a_1\left[\exp\left(-\frac{(\Delta H - a_2)^2}{2a_3^2}\right) + \exp\left(-\frac{(\Delta H + a_3)^2}{2a_3^2}\right)\right] \quad (1)$$

where $\Delta H = H - H_0$, H is the applied magnetic field and H_0 the value of H at the centre of the doublet, i.e., it consists of the superposition of two identical Gaussian line shapes whose centres are separated by an interval $2a_2$ and whose individual second moment about their centre is a_3^2. The area under this composite curve is $(8\pi)^{1/2}a_1a_3$ and the second moment is $\langle \Delta H_2 \rangle = a_2^2 + a_3^2$. This line shape was fitted to the outer part of the experimental line with a_1, a_2 and a_3 as adjustable parameters using a least squares procedure. It was found that the search for the best overall fit did not depend on choosing initial values for the parameters a_1, a_2, and a_3, once the range of the outer part of the absorption line was determined. Then the only difficulty was that the a_n values obtained by best fit depended on the portion of the outer part of the absorption line that had been chosen for fitting. It can be easily understood that the wider the ranges chosen, the more precise the fitting would be. However, if the range chosen is too wide and the non-crystalline component peak at the centre is involved, we can never get a satisfactory fit. Therefore, a range of a_n values was obtained by the best overall fit using different ranges of the outer part of the absorption line. Gaussian doublets fitted in the range 29–50 kHz were found to be optimal for the samples of the original and compacted SPECTRA 1000 fibre.

3. Results and discussion

3.1. Shrinkage of the original SPECTRA fibre

The temperature dependence of the shrinkage of the SPECTRA 1000 fibre is plotted in Fig. 1. With increasing temperature, the shrinkage of the fibre increases very slowly, being lower than 10% until the temperature reaches 140 °C. As soon as the temperature passes 140 °C, the shrinkage increases rapidly and reaches its maximum value very quickly. This pattern of shrinkage behaviour is typical of both gel spun and melt spun drawn polyethylene fibres [11, 12]. In both types of fibre the crystalline morphology constrain the structure so that substantial shrinkage is only observed when the melting range is reached and there is sufficient mobility for the molecular chains to slide within the crystalline regions. It is worth noting that the majority of the compaction temperatures used in this study (142–156 °C) are above the point at which full shrinkage of the fibre would be expected to have occurred. Therefore during the initial "low pressure" stage of compaction, sufficient pressure is required to restrain the fibres from shrinking and losing orientation. At the same time it is clear from our work on other fibres that optimum compaction is achieved using a two stage process with as low a first stage pressure as possible. A balance is therefore required between these two conflicting requirements.

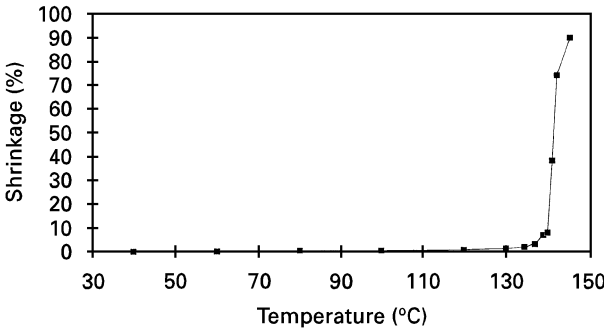

Figure 1 The temperature dependence of shrinkage rate for the SPECTRA PE fibre.

3.2. Melting behaviour

3.2.1. Original fibre

In our previous work on the hot compaction of various melt processable polymer fibres, DSC measurements, on both the original fibre and on the compacted fibre composites, have proved helpful in identifying the compaction mechanisms. DSC studies were therefore undertaken on the SPECTRA 1000 fibre and the compacted SPECTRA composites.

The normalized DSC thermogram of the original fibre is shown in Fig. 2, together with that of the same fibre after cooling and subsequent reheating, measured in order to ascertain the position of the melting peak of melted and recrystallized material, such as might be produced during compaction. The original fibre can be seen to show a double melting peak, which is not unusual for a very highly crystalline gel spun polyethylene fibre. For a review of work before 1980 on highly oriented materials produced from solution, and resolution of many ambiguities, the reader is referred to Wunderlich [13]. It is now generally understood that in such materials the higher melting peak is due to the formation of a hexagonal crystalline phase during melting. The development of this phase prior to melting has been shown by X-ray measurements on constrained ultradrawn PE fibres [14, 15], and it has been demonstrated to be the same as that formed by high pressure annealing [16].

A second complication is seen when we study the effect of constraint on the melting behaviour of the fibre. The melting behaviour of the free fibre, the partially constrained fibre, and the fully constrained fibre are compared in Fig. 3; large differences are seen in the melting behaviour under these three constraint conditions. As expected, the free fibre has the lowest melting point, 146.7 °C and the fully constrained fibre the highest, 156.9 °C. Double melting peaks appear on the thermograms for all the three samples. The relative area of the double peaks changes depending on the type of constraint. The increase in melting temperature of the main peaks, induced by constraint of the fibre, amounts to 10.2 °C.

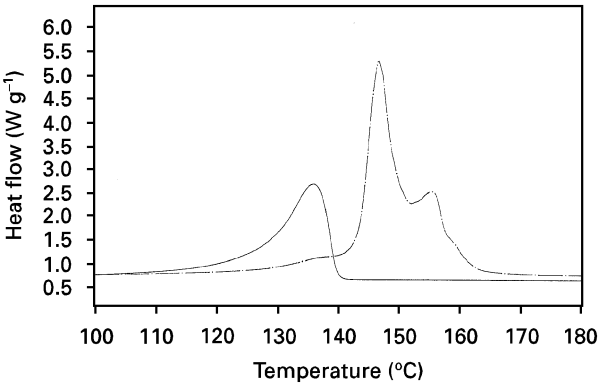

Figure 2 DSC thermograms of the original fibre (—·—) and the same fibre after cooling and reheating (——).

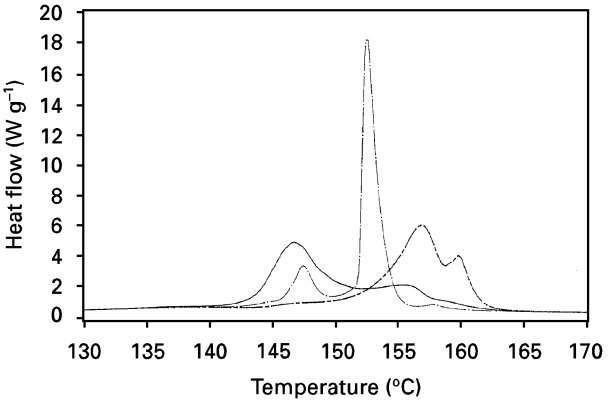

Figure 3 DSC thermograms of original fibres detected at unconstrained (——); partially constrained (—·—); and fully constrained state (— — —).

3.2.2. Compacted materials

Typical DSC thermograms of the hot-compacted materials are shown in Fig. 4, and the melting points and enthalpy of fusion determined from the DSC curves for the materials compacted at different temperatures are shown in Fig. 5. The samples compacted at 142 and 153 °C show very similar DSC thermograms consisting of a single melting peak with a small shoulder at a lower temperature. Interestingly the higher melting peak seen in the melting of the original fibre due to the formation of a hexagonal phase, is not seen in the melting of the compacted materials. This suggests that in the compacted materials the constraint on individual fibres may not be high enough to raise the melting point sufficiently to allow the hexagonal phase to form before melting.

The small low temperature peak for the compacted materials is at a similar position to that expected for melted and recrystallized material (as shown in Fig. 2), although the melting behaviour of the original fibre, also shown in Fig. 2, reveals a similar small shoulder at this position. The DSC experiments therefore do not indicate any substantial fibre melting occurring below 153 °C. The melting point and heat of fusion for all the samples compacted in the temperature range of 142–153 °C are nearly constant (see Fig. 5), indicating that the fibre has changed very little when compacted at these temperatures. When the fibre was compacted

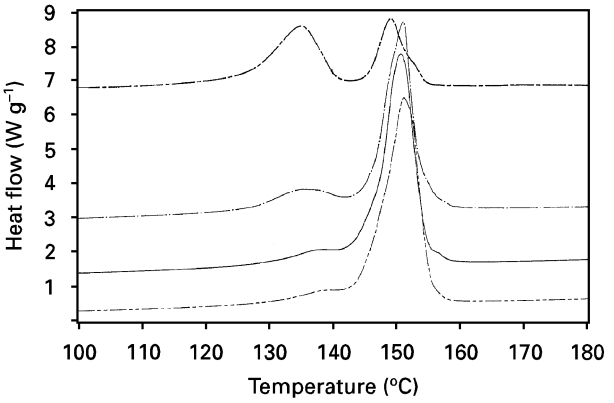

Figure 4 DSC thermograms of the samples compacted at 142 °C (— — — —), 153 °C (——), 154 °C (—·—), 155 °C (— — —).

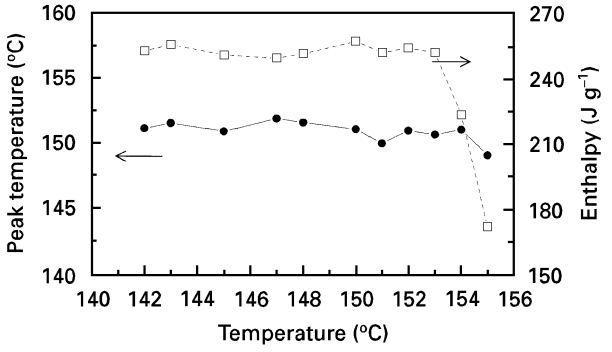

Figure 5 Dependence of the peak melting temperature (□) and enthalpy of melting (●) on the compaction temperature.

at 154 °C, the shoulder on the melting curve becomes larger, indicating that a small fraction of the fibres had melted and recrystallized during the hot-compaction process. Drastic changes in the DSC thermograms occurred only when the compaction temperature was increased from 154 to 155 °C. A different thermogram with two well separated melting peaks was observed for the 155 °C materials. Both the total heat of fusion and the melting point of the peak at higher temperature were much lower for this sample than the others (Fig. 5). The first peak on the DSC curve of the 155 °C material had a melting point of 135.4 °C, the same as the melting temperature of melted material (Fig. 2), while the reduced heat of fusion results from a lower degree of crystallinity of the new species produced by melting and recrystallization during hot-compaction. It is worth noting that the temperature range over which significant fibre melting occurs is very narrow.

3.3. Bending properties of compacted material

To study the mechanical properties, the compacted materials were cut either along the fibre direction (the longitudinal) or perpendicular to the fibre direction (the transverse) and the flexural modulus and strength of each specimen was measured at room temperature. As with the previous studies we have concentrated on measuring the trade-off between the longitudinal

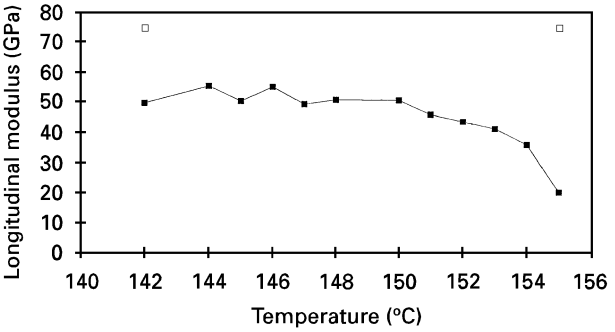

Figure 6 Dependence of the longitudinal modulus of the samples on compaction temperature. (■) compacted, (□) original fibre.

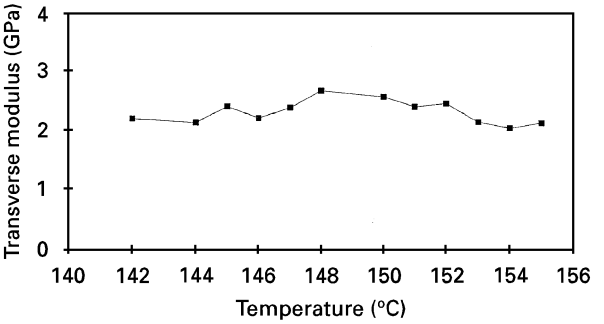

Figure 8 Transverse flexural modulus versus compaction temperature.

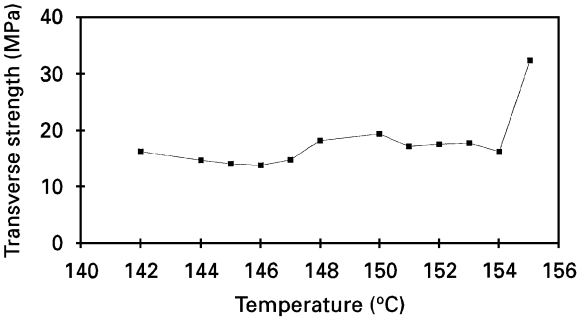

Figure 7 Transverse flexural strength versus compaction temperature.

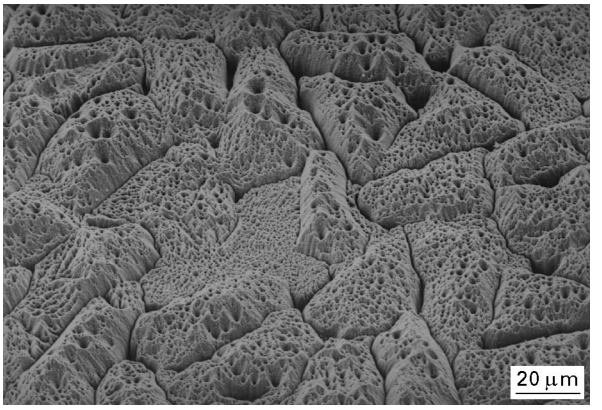

Figure 9 Scanning electron micrograph of an etched transverse surface for a sample compacted at 148 °C.

modulus, which is determined by the properties and proportion of the original fibre structure, and the transverse strength which is developed at the expense of the original fibre (and hence the longitudinal modulus).

The dependence of the longitudinal flexural moduli of the samples on the compaction temperature is shown in Fig. 6. The tensile modulus of the original fibre is also plotted in Fig. 6. Increasing the compaction temperature from 142 to 150 °C, the longitudinal modulus does not change significantly but it decreases after 150 °C, especially for the increase from 154 to 155 °C. There is no sharp maximum in the longitudinal modulus curve, which is very different from the results for the melt-spun PE fibre [1]. In addition, the modulus decrease induced by hot-compaction, from 74.7 GPa for the original gel-spun fibre to *ca* 50 GPa for the materials compacted in the range of 142–150 °C, is more than 25%, which is greater than the 10% fall for the material compacted from melt-spun PE at the optimum temperature of 138 °C [1].

The transverse strength and transverse modulus values for each compacted material are plotted versus the compaction temperature in Figs 7 and 8, respectively. In the temperature range of 142–154 °C, the transverse strength is relatively constant. When the temperature is increased from 154 to 155 °C, there is a sharp increase in the transverse strength, indicating that a greater fraction of the fibre had melted at this temperature. In Fig. 7, we see that the transverse modulus does not change significantly over the whole temperature range of 142–155 °C.

3.4. Morphological observations

SPECTRA fibres are known to contain longitudinal density deficient regions, similar to those in TENFOR fibres, which give rise to conical pits on etching [2]. In earlier work with a diamond knife [17], a transverse section was taken from a sample compacted at 148 °C and etched. Fig. 9 shows this surface, in a tilted view at 45 ° to the fibre direction. This shows many similarities to etched surfaces of TENFOR fibres compacted at 134 °C [3], in that the fibres have deformed to largely fill the space, except at corners where there are open channels. The surface where the fibres meet are also open enough to have allowed some penetration of etchant, and a chamfered profile has developed inwards from the fibre boundaries. The interior of the fibres is likewise full of small conical pits formed by etching around density-deficient regions, but they are more numerous and irregular in distribution than in the TENFOR fibres.

In the present work, morphological analysis has been carried out on samples compacted at 144, 148, 154 and 155 °C. We have used a glass knife on these samples to cut surfaces at 45 ° to the main fibre axis. Etched diagonal surfaces of these samples viewed down the fibre axis are shown in Fig. 10(a–d). The features observed fall under two headings, the compaction between the fibres, and the internal structure of the fibres. In both categories, the materials compacted at 144, 148, and 154 °C have many features in common, and the 155 °C material is quite distinct.

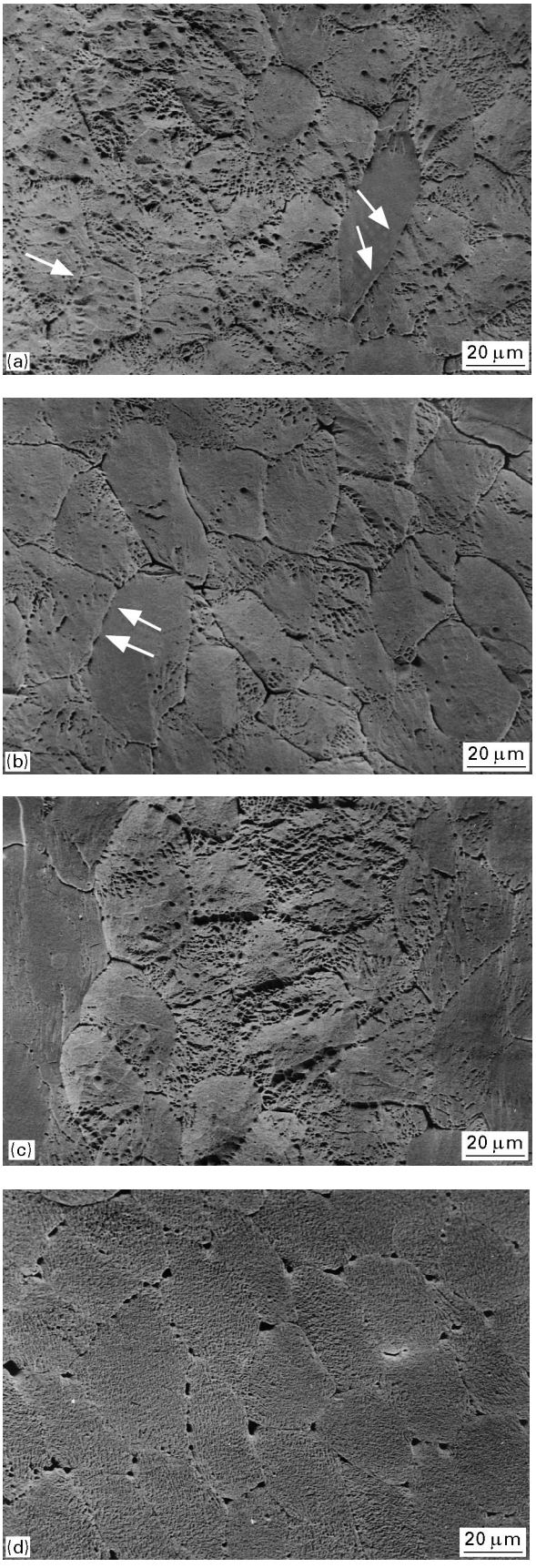

Figure 10 Scanning electron micrograph of etched diagonal surfaces viewed down the fibre axis for samples compacted at (a) 144 °C, (b) 148 °C, (c) 154 °C and (d) 155 °C.

Regarding the compaction process, the original SPECTRA fibres have cross-sections in the shape of very irregular polygons, and when they are crushed together with no intervening melt these polygons deform so as to fill most of the available space. At 144 and 148 °C, some inter-particle boundaries remain appearing as narrow gaps, whereas in some others the fibres appear to have partly welded together with rows of "welding points" visible along the gaps. The 154 °C material is not significantly different, but the gaps appear to be narrower and to have sealed in certain places. The polygonal shapes are most easily discerned in the materials compacted at 148 °C, but this is a result of less etching of the internal structure in this instance, rather than any difference between the compactions.

At 155 °C the appearance has changed greatly. The fibres have softened and distorted into much smoother polygons with fewer sides. Moreover, the inter-particle boundaries are much less distinct, except where they are marked by rows of voids; larger interstitial voids have formed where three or sometimes four fibres meet. Even though the fibres may have melted to some degree, there is no evidence of a supply of melt which can fill the gaps, as there was with TENFOR PE compacted at 138 °C [2]. Under those circumstances the TENFOR fibres retained their circular cross-sections, but at lower temperatures, where melt was in short supply, they deformed into polygons to fill the spaces [3]. However, the appearance here is much more like compacted polypropylene fibres, where the fibres have softened and deformed but what melting may have occurred inside the fibres has not provided material external to the fibres to fill the gaps between fibres [6].

The most drastic morphological changes occur between 154 and 155 °C, which is in agreement with the above DSC and mechanical measurements, but the foregoing would leave the impression that little morphological change at all happens between 144 and 154 °C. This is mainly because the view down the fibres telescopes the perspective of the inter-fibre boundaries. However, examining the etched external longitudinal surfaces (not cut) of the same specimens in a reflection optical microscope gives a more comprehensive picture. In the 144 °C material the etchant is seen to have easily penetrated between the fibres, and in the top layer or two these fibres have been narrowed by etching into more rounded cross-sections, and isolated from each other. At higher compaction temperatures, the fibres are etched as a uniform block, with some widening of the gaps between them in the 148 °C material, much less so for 154 °C, and for 155 °C the gaps are hardly discernible, showing that there is a progressive increase in lateral connectivity.

The effect of etching on the internal structure of the fibres is not uniform. In the micrograph of the 154 °C material (Fig. 10c), the central band of fibres displays many small craters in each fibre, which are similar in origin to those observed in TENFOR fibres [3], in that they occur where the etchant has opened out a conical hole around a narrow density deficient region extending along the fibre direction. It is known [18, 19] that individual SPECTRA fibres contain such regions even without thermal treatment or compaction, as do TENFOR fibres, which behave similarly on etching. However, the fibres to left and right do not display craters,

those to the left in particular having a smeared appearance (Fig. 10d). The difference observed here is believed to arise from the cutting on the microtome, rather than in the compaction process. Compacted SPECTRA fibres are somewhat tougher than DYNEEMA. Blocks of the latter can be cut with a glass knife at 45° and still give a good surface for etching [17]. With SPECTRA, the edge of the glass knife is damaged even after one cut, so there is a tendency to smear out the fibre cut surface, and so close off the density deficient regions to the exclusion of etchant. Nevertheless, the central region of Fig. 10d appears to have been cut with a part of the knife which had survived relatively undamaged.

Taking these factors into account, one can be confident that the original density deficient structure of the fibres survives largely unchanged during the compaction process up to 154 °C. At 155 °C, the internal structure of the fibre is greatly modified. Because the toughness of the fibres has dropped, this specimen could be cut cleanly with a glass knife, and in Fig. 10d we see a fair representation of the internal structure as modified by etching. The appearance is now much more like that of compacted polypropylene [6]. The original structure of long density deficient regions has disappeared, and been replaced by a structure with orientation in two visible directions.

3.5. A comparison of the DSC, SEM and mechanical properties

All the results of the DSC and SEM investigations are consistent with the mechanical tests. If the fibres are compacted in the range of 142–154 °C, there is no evidence of significant surface melting. Therefore, all the resultant compacted composites have similar morphologies and mechanical properties. In addition the peak melting temperatures (Fig. 5) of the compacted materials are very similar and close to that of the partially constrained fibre, 152.6 °C (Fig. 3). When the compaction temperature is increased to 155 °C, there is evidence that to some extent the fibres have melted and recrystallized from the continuous fibre crystals into a new form of lamellar crystals during the process of hot compaction. Therefore, we observed the appearance of the lower melting peak in Fig. 4 and the different morphology (Fig. 10d) for the 155 °C material. The heat of fusion of this sample is much lower due to the decrease in total crystallinity. The melting and recrystallization of the fibres results in a large decrease in the longitudinal modulus of the compacted material (Fig. 6). The SEM pictures suggest that at this highest temperature the changes in the morphology due to melting occur throughout the fibre, rather than just at the fibre surface, which results in a large increase in the transverse strength of the composites (Fig. 7).

While broadly constant, there are small differences in the mechanical properties (Figs 6–8) of the composites in the temperature range 142–153 °C, even though the DSC results indicate that all of the samples have similar melting behaviour (Figs 4 and 5). Over the temperature range 142–153 °C, the unidirectionally arranged fibres do not melt, but do develop a reasonable transverse strength by a combination of mechanical interlocking of, and intermittent fusion at, the fibre surfaces. At the higher temperatures, the fibres become softer, such that they can achieve a higher degree of coherence among them so as to increase the surface contact areas. The welding points are thus able to be distributed more evenly, although they do not seem to become much more abundant. Taken in bulk, therefore, the materials compacted at higher temperature show only a small increase in transverse strength and modulus. But local weaknesses are removed by the greater evenness of the bonding, and this manifests itself in cutting behaviour. Application of a glass knife or a steel razor blade longitudinally to the 144 °C specimen results in extensive pulling out of fibres: less so for 148° and much less for 154° specimens.

The fall of the longitudinal modulus of the gel-spun fibre compared with the original fibre, results from a combination of macroscopic misorientation due to alignment problems in arranging the fibres in the mould, non-perfect coherence among the fibres, and a possible decrease in the modulus of the fibre induced by annealing. Although little melting and recrystallization occurs during compaction of the fibres in the range 142–154 °C, there is a tremendous annealing effect on the materials, which has been confirmed by the following discussion on the broad-line NMR results. Comparing the gel-spun fibre with the previous work on the melt-spun fibre [1], we find that for the optimum compaction conditions the compacted materials from the two types of fibres have similar values for both the transverse strength and longitudinal modulus. Although the decrease in the longitudinal modulus induced by hot-compaction is greater for the gel-spun fibre compared with the melt-spun fibre, the gel-spun fibres start with a higher modulus.

3.6. Broad-line NMR results

For all the broad-line NMR measurements the main fibre direction was aligned parallel to the applied magnetic field. Fig. 11a shows the derivative spectrum for the original SPECTRA fibre, while Fig. 11b shows the corresponding absorption spectrum. The absorption spectrum shows a clear Gaussian doublet, with a small peak at the centre which can be attributed to machine effects. Initially, we attempted to neglect just the sharp peak at the centre and fit the whole spectrum using the Gaussian doublet line shape described by Equation 1. However this did not result in the best possible fit, which was obtained by fitting only the outer part of the curve as described above in section 2.6. The fitted curve is shown in Fig. 11a, and the values of a_1, a_2 and a_3 obtained from this fit are listed in Table 1.

Fig. 12(a–d) show the derivative spectra and Fig. 13(a–d) the corresponding absorption spectra and the best fit curves for the samples compacted at 144°, 148°, 154° and 155 °C. For the compacted materials the line shape is different to the original fibres, and is similar to that seen for typical PE samples [20]. It is clear that the spectra are a composite and the direct interpretation is that a broad doublet due to

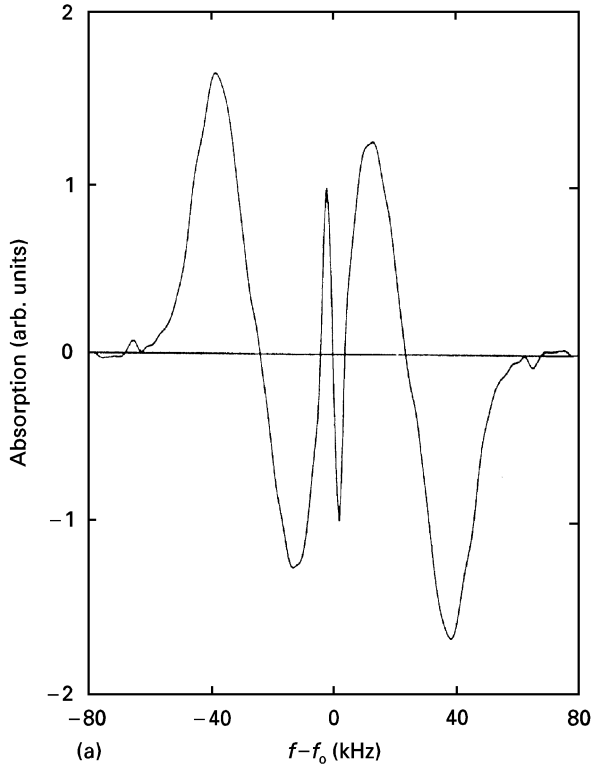

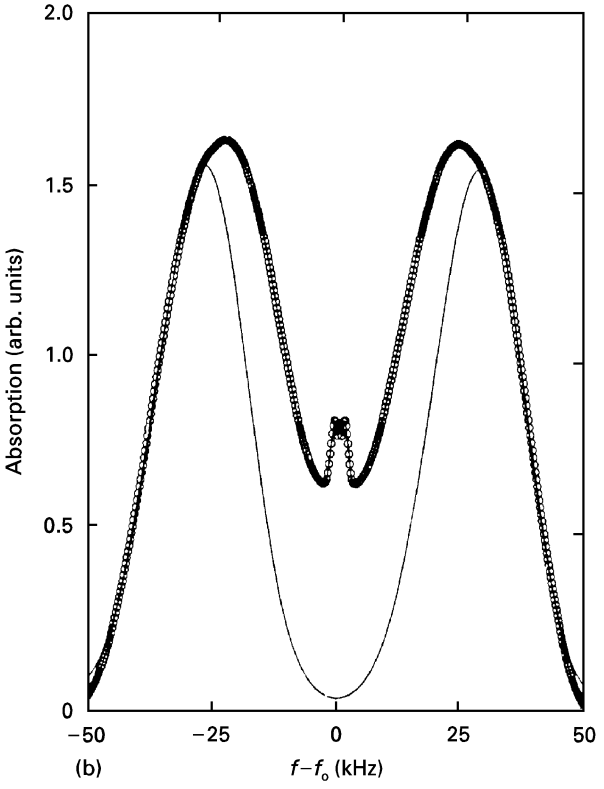

Figure 11 Broad-line NMR spectra of the original SPECTRA fibre, (a) the derivative spectra (b) the absorption spectra.

a rigid phase, is superposed on a narrower singlet from a more mobile phase. The intensity of the broader doublet is gradually reduced relative to the narrow component as the compaction temperature is increased.

The proportions of rigid and mobile material can be determined from the fitting of the Gaussian doublet. The rigid mass fraction, f_R, is given by the ratio of the integrated intensity of the rigid fraction component (the fitted Gaussian doublet) to the total integrated intensity. The mass fraction of the mobile component is, in this case, the complement of the rigid mass fraction. Fitting parameters for the Gaussian doublet, rigid fraction values, f_R, in comparison with the DSC crystallinity, W_c, are listed in Table 1.

TABLE I Fitting parameters for Gaussian doublet and rigid fraction values f_R

Samples	a_1	a_2	a_3	f_R	W_c
Spectra fibre	0.016	27.8	8.93	0.695	0.801
Compacted at 144 °C	0.01	28.7	8.65	0.436	0.863
Compacted at 148 °C	0.0098	29	8.48	0.414	0.86
Compacted at 154 °C	0.009	27.6	8.96	0.401	0.764
Compacted at 155 °C	0.0085	25.8	8.81	0.374	0.588

All the values of the rigid fraction, f_R, of the samples determined by the broad-line NMR technique are lower than the DSC crystallinity. In two recent studies of ^{13}C NMR of polyethylene [21, 22], crystalline fractions of 0.632, 0.76, and 0.85 were observed for different molecular weight samples of gel-spun PE fibres. Compared with those values, the rigid fraction of the SPECTRA 1000 fibre determined from broadline NMR of 0.695, shown in Table 1, is reasonable. In another recent publication, Fu *et al.* [23] measured the DSC crystallinity, W_c, to be 0.82 and the rigid fraction, f_R, by ^{13}C NMR to be 0.73. These values again agree very well with those determined here for W_c and f_R (Table I) of the original fibre of 0.80 and 0.695 respectively. It is not too surprising that the quantitative measure of the crystalline phase may be somewhat different depending on the particular NMR technique used, and the molecular weight of the fibre.

Another interesting aspect shown in Table I is that all the values of the rigid fraction, f_R, for the compacted materials are much lower than that of the original fibre and they decrease gradually with increasing compaction temperature. The values of the DSC crystallinities for the compacted materials also fall with increasing compaction temperature, although the difference between the NMR and DSC crystallinities for the compacted materials is larger than the difference in these two values for the original fibre.

The DSC crystallinity, W_c, the NMR rigid fraction, f_R, and the difference between them, $f_M = W_c - f_R$, are plotted in Fig. 14 as a function of the compaction temperature. In the work of Fu *et al.* [23] the difference, f_M, between the DSC crystallinity, W_c, and the NMR crystallinity, f_R, was attributed to an intermediate oriented amorphous phase. It was shown that the formation of the intermediate phase was a consequence of the high levels of orientation in the fibre causing the chains to align, to have a largely trans configuration and to be ordered preferentially parallel to the fibre axis. In this way they could show a small heat of fusion, but in view of their increased mobility compared to the true crystalline regions it would not contribute to the rigid crystalline fraction, f_R determined by NMR.

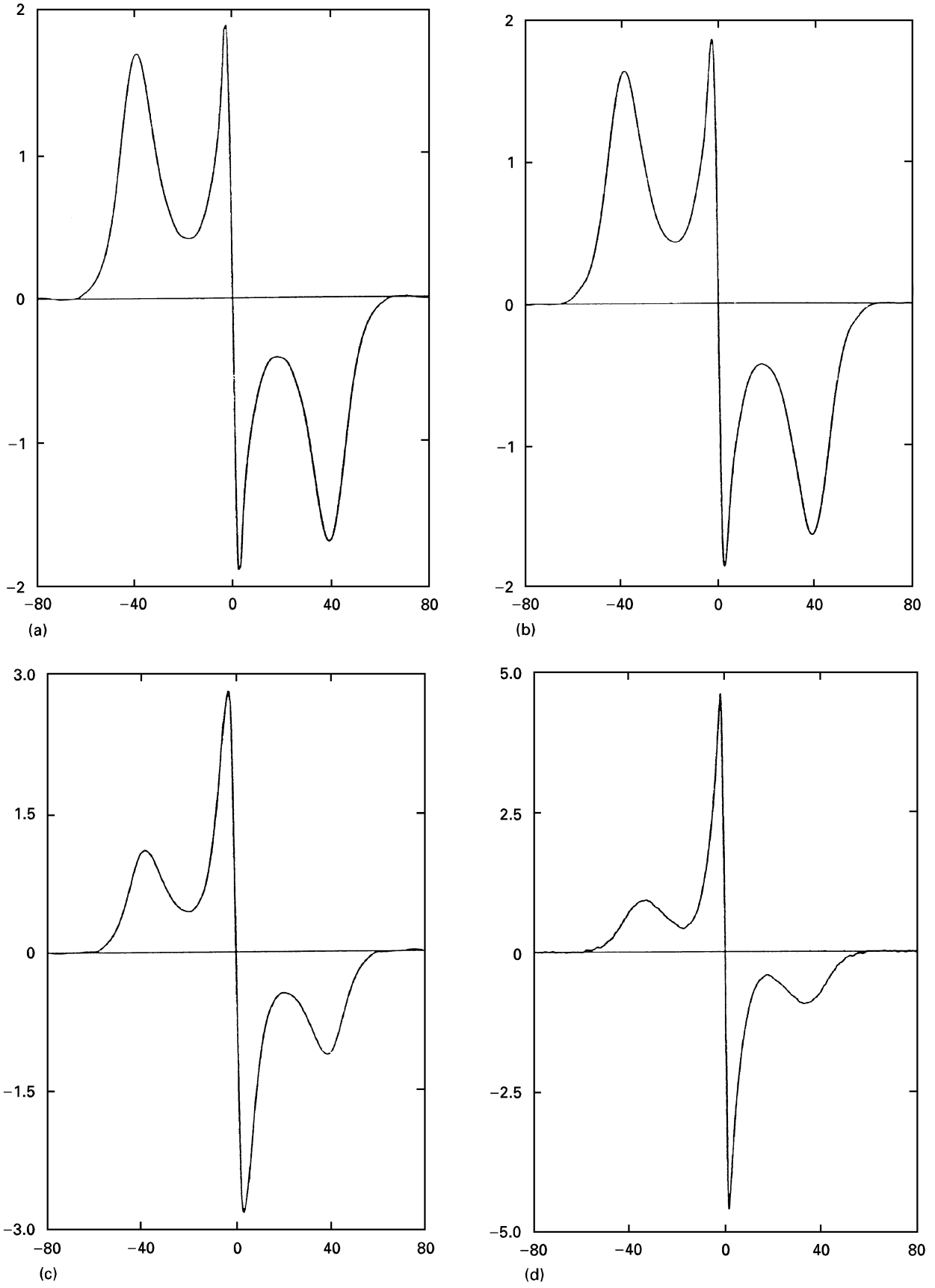

Figure 12 Derivative broad-line NMR spectra for materials compacted at (a) 144 °C, (b) 148 °C, (c) 154 °C and (d) 155 °C. The abscissae are in kHz and the ordinates represent absorption derivative normalized to unit integrated intensity.

Peterlin and Meinel [24] and Meinel and Peterlin [25] considered the heat of fusion of the non crystalline or amorphous regions of cold drawn quenched polyethylene films and concluded that the DSC heat of fusion, ΔH, for the oriented polymer could be written as:

$$\Delta H = f_R \Delta H_c + f_M \Delta H_M \quad (2)$$

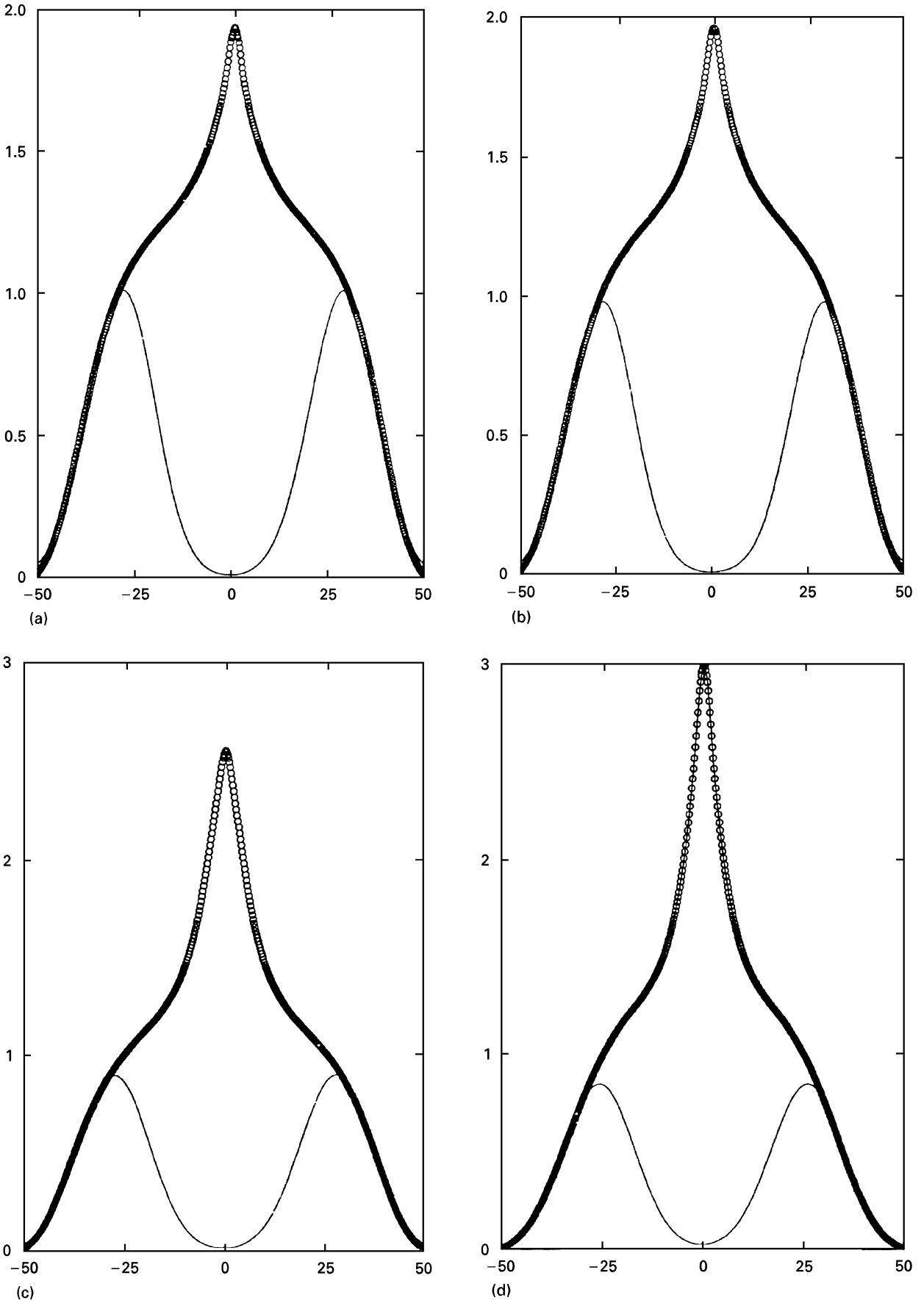

Figure 13 NMR absorption spectra for materials compacted at (a) 144 °C, (b) 148 °C, (c) 154 °C and (d) 155 °C. The abscissae are in kHz and the ordinates represent absorption normalized to unit integrated intensity.

where ΔH_c is the heat of fusion of the crystalline regions and ΔH_M is the heat of fusion of the oriented amorphous regions. Values of between 0.12 and 0.20 were determined for the non crystalline fraction of a range of gel spun polyethylene fibres. In the two-dimensional ^{13}CCP/MAS NMR study of Tzou *et al.*

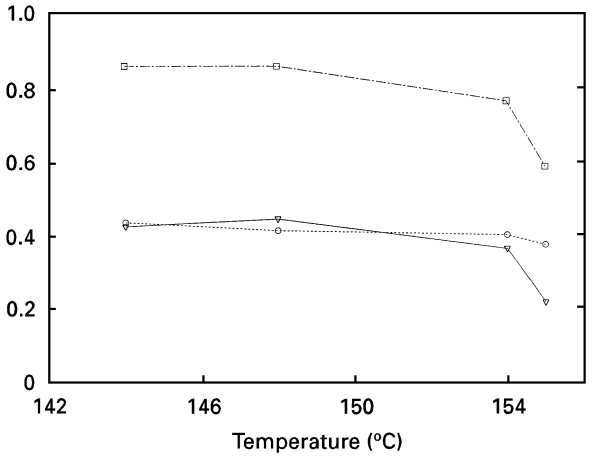

Figure 14 Plots of: (○) NMR rigid fraction f_R, (□) DSC crystallinity W_c, and (▽) the difference $f_M = W_c - f_R$ versus compaction temperature.

[22], the oriented mobile components described as C1 are 0.15 and 0.06 for their gel-spun PE fibres, PE-I and PE-II. A much higher value of oriented mobile component, 0.34 was measured for a sample of gel-spun fibre SPECTRA 2000 by Chen *et al.* [21] using the ^{13}C NMR technique. The oriented mobile component f_M, of our sample of SPECTRA 1000 is equal to 0.106 (from Table I), and it becomes much greater in the compacted materials, from 0.427 to 0.214 depending on the compaction temperature.

The change in the longitudinal modulus of the fibre due to compaction correlates much better with the change in the rigid fraction, f_R, rather than the DSC crystallinity, W_c. The ratio of the longitudinal modulus of the compacted material at 144 °C to the original fibre is 0.66 (50/70) which closely agrees with the value of f_R of 0.63 (0.436/0.695) from the broadline NMR measurements. A similar comparison using the DSC crystallinity, W_c, does not correlate as well with the change in the longitudinal modulus. It is likely that the longitudinal fibre modulus is more affected by the size and fraction of the crystalline regions, and it is this that is directly measured by broadline NMR.

To summarize the results of the compaction experiments, SPECTRA 1000 gel spun polyethylene fibres can be successfully compacted. The major difference with this fibre is that samples of reasonable mechanical properties can be manufactured over a *wide* temperature range *below* the onset of melting, whereas the compaction of melt spun fibres previously studied has involved processing the fibres *within* their melting range (usually a *narrow* temperature window). With the gel spun fibres the main melting range is so narrow, especially under constrained conditions, that samples cannot be made controllably within this temperature window.

The mechanism of fibre to fibre bonding in the compacted gel spun composites is found to be not through selective surface melting and "melt bonding", but through spot welding at numerous junctions along the interlocked irregular polygonal shapes of the fibres. While this does not develop as high a transverse strength as the melt bonding seen in compacted melt processable fibres, it is less temperature sensitive and therefore easier to control.

Although for compaction temperatures lower than 154 °C no obvious melting and recrystallization occurs, as revealed by DSC and SEM observations in Figs 4 and 9, there is still a loss of fibre properties compared to the original fibre. As indicated by the broad-line NMR measurements, almost half of the orthorhombic crystalline material in the original fibre has transformed into the oriented mobile material after compaction (Fig. 13(a–d)). Especially in the process of hot-compaction, the fibres are annealed in an almost but not fully constrained state. Melting at constant length prevents the chains from adopting random coil conformations. Only then could many molecular chains, being originally crystalline, become relaxed oriented (oriented mobile) chains due to the high temperature annealing. Although the oriented mobile molecules will undoubtedly contribute to the longitudinal modulus, the contribution is certainly much less than was the case when they were orthorhombic crystals. It is this microstructural transformation, induced by annealing the constrained fibre, that causes the decrease in the longitudinal modulus after compaction.

4. Conclusions

Gel-spun SPECTRA 1000 fibre has been successfully compacted to produce a homogeneous product with a reasonable longitudinal modulus and a transverse strength sufficient for useful application. As a result of the continuous fibrillar crystal structure of the gel-spun fibre, the mechanical properties and morphology of the resultant compacted fibre composites show little change in the temperature range 144–154 °C. Evident melting and recrystallization occur only if the fibres are compacted at the high temperatures, such as 155 °C, which is close to the melting point of the fully constrained fibre. The main feature in the morphology of the compacted materials are well-packed irregular polygons with some "welding points". Compared with the hot-compaction of melt-spun fibre, the loss in original fibre modulus is much greater because a considerable amount of crystalline material has transformed to oriented mobile chains. However the higher modulus of the gel spun fibre has the consequence that under certain conditions the final properties of the compacted gel spun fibre composite are very similar to those of a compacted composite produced from melt spun fibre.

Acknowledgements

R. J. Yan gratefully thanks the Royal Society, London, for the provision of a research fellowship. Acknowledgement is also made to colleagues at Leeds University for experimental assistance and helpful discussion. J. Teckoe is thanked for his assistance in preparing samples for etching.

References

1. P. J. HINE, I. M. WARD, R. H. OLLEY and D. C. BASSETT, *J. Mater. Sci.* **28** (1993) 316.

2. R. H. OLLEY, D. C. BASSETT, P. J. HINE and I. M. WARD, *Ibid* **28** (1993) 1107.
3. M. A. KABEEL, D. C. BASSETT, R. H. OLLEY, P. J. HINE and I. M. WARD, *ibid* **29** (1994) 4694.
4. *Idem*, *ibid* **30** (1995) 601.
5. J. RASBURN, P. J. HINE, I. M. WARD, R. H. OLLEY, D. C. BASSETT and M. A. KABEEL, *ibid* **30** (1995) 615.
6. M. I. ABO El-MAATY, D. C. BASSETT, R. H. OLLEY, P. J. HINE and I. M. WARD, *ibid* **31** (1996) 1157.
7. A. J. PENNINGS, J. M. A. A. van der MARK and A. M. KIEL, *Kolloid Z. Z. Polym.* **237** (1970) 336.
8. R. H. OLLEY and D. C. BASSETT, *Polymer* **23** (1982) 1707.
9. J. CLEMENTS, G. R. DAVIES and I. M. WARD, *ibid* **26** (1985) 208.
10. H. PRANADI and A. J. MANUEL, *ibid* **21** (1950) 303.
11. R. J. YAN, Y. LUO and B. JIANG, *J. Appl. Polym. Sci.* **47** (1993) 789.
12. G. CAPACCIO and I. M. WARD, *Colloid and Polym. Sci.* **260** (1982) 46.
13. B. WUNDERLICH, in "Macromolecular physics", Vol. 3: "Crystal melting", (Academic Press, New York, 1980), section 9.3.1.1.
14. A. J. PENNINGS and A. ZWIJNENBURG, *J. Polym. Sci. Polym. Phys. Edn* **17** (1979) 1011.
15. N. A. J. M. van AERLE and P. J. LEMSTRA, *Polym. J.* **20** (1988) 131.
16. S. TSUBAKIHARA, A. NAKAMURA and M. YASUNIWA, *ibid* **23** (1991) 1317.
17. M. I. ABO El-MAATY, M. A. KABEEL, D. C. BASSETT, R. H. OLLEY, P. J. HINE and I. M. WARD, *J. Mater. Sci.* **31** (1996) 1157.
18. M. I. ABO El-MAATY, R. H. OLLEY, D. C. BASSETT, P. J. HINE and I. M. WARD, presented at Physical Aspects of Polymer Science meeting, University of Reading (1993).
19. M. I. ABO El-MAATY, *PhD thesis*, University of Mansoura, Egypt (1994).
20. P. G. KLEIN, *Nexus Newsletter*, Spring Issue, (1995) 2.
21. W. CHEN, Y. FU, B. WUNDERLICH and J. CHEN, *J. Polym. Sci. Part B: Polym. Phys.* **32** (1994) 2661.
22. D. L. TZOU, T. H. HUANG, P. DESAI and A. S. ABHIRAMAN, *ibid* **31** (1993) 1005.
23. Y. FU, W. CHEN, M. PYDA, D. LONDONO, B. ANNIS, A. BOLLER, A. HABENSCHUSS, J. CHENG and B. WUNDERLICH, *J. Macromol. Sci.-Phys.* **B35** (1996) 37.
24. A. PETERLIN and G. MEINEL, *Polym. Lett.* **3** (1965) 783.
25. G. MEINEL and A. PETERLIN, *J. Polym. Sci.* **B5** (1967) 613.

Received 11 July 1996
and accepted 7 April 1997